

# Magnetic and calorimetric studies of double perovskites $Ba_2LnReO_6$ ( $Ln = Y, Nd, Sm-Lu$ )

Yoshinori Sasaki, Yoshihiro Doi and Yukio Hinatsu

Division of Chemistry, Graduate School of Science, Hokkaido University, Sapporo, 060-0810, Japan

Received 16th January 2002, Accepted 22nd May 2002

First published as an Advance Article on the web 27th June 2002

The perovskite-type compounds  $Ba_2LnReO_6$  ( $Ln = Y, Nd, Sm-Lu$ ) have been synthesized. Powder X-ray diffraction measurements and Rietveld analysis show that they are monoclinic with space group  $P2_1/n$  and that  $Ln^{3+}$  and  $Re^{5+}$  ions are structurally ordered. Anomalies are found in their magnetic susceptibility and specific heat measurements, which suggest an antiferromagnetic ordering of  $Re^{5+}$  ions for  $Ba_2LnReO_6$  ( $Ln = Y, Nd, Sm, Gd-Ho, Lu$ ) and that of  $Tb^{3+}$  ions for  $Ba_2TbReO_6$ .

## Introduction

The perovskite-type oxides have the general formula  $ABO_3$ , in which  $A$  represents a large electropositive cation and  $B$  represents a small transition metal ion. The perovskite structure can be described as a framework of corner-shared  $BO_6$  octahedra which contain  $A$  cations at 12-coordinate sites. Double perovskite-type oxides have the formula  $A_2B'B''O_6$ , in which the primes indicate the different ions in different oxidation states, and the cations at the  $B$  sites,  $B'$  and  $B''$ , are regularly ordered, *i.e.*, 1:1 arrangement of  $B'$  and  $B''$  ions has been observed over the six-coordinate  $B$  sites. Since the  $B$  cations generally determine the physical properties of perovskites, different kinds of  $B'$  and  $B''$  ion should show a variety of the physical properties of double perovskite oxides.

We have been studying preparation, crystal structure and magnetic properties of double perovskite oxides,  $Ba_2LnNbO_6$ ,<sup>1</sup>  $Ba_2LnTaO_6$ ,<sup>2,3</sup>  $Ba_2LnRuO_6$ ,<sup>4,5</sup> and  $Ba_2LnIrO_6$ ,<sup>6,7</sup> where  $Ln$  represents a rare earth ion. Through studies on  $Ba_2LnNbO_6$  and  $Ba_2LnTaO_6$  in which both  $Nb^{5+}$  and  $Ta^{5+}$  ions are diamagnetic, these compounds are paramagnetic down to 4.2 K and their magnetic properties are characterized by the behavior of  $Ln^{3+}$  ions in the double perovskites.<sup>1-3</sup> The electronic structure of  $Ru^{5+}$  is  $[Kr]4d^3$  ( $[Kr]$ : krypton electronic core). Such highly oxidized cations from the second or third transition series sometimes show quite unusual magnetic behavior. So, the ordered perovskites  $Ba_2LnRuO_6$  are expected to show interesting magnetic properties at low temperatures. Most of the  $Ba_2LnRuO_6$  compounds show antiferromagnetic transitions at 15–30 K. From the neutron diffraction measurements on  $Ba_2PrRuO_6$ <sup>4</sup> and  $Ba_2NdRuO_6$ ,<sup>5</sup> their magnetic structures are determined to be of Type I. In the above-mentioned  $Ba_2LnMO_6$  ( $M = Nb, Ta, Ru$ ) compounds, lanthanide and  $M$  ions are in the trivalent and pentavalent states, respectively. Magnetic susceptibility and specific heat measurements on iridium compounds  $Ba_2LnIrO_6$  show that they are paramagnetic down to 1.8 K except for the Ce and Pr compounds.<sup>7</sup> Both the  $Ba_2CeIrO_6$  and  $Ba_2PrIrO_6$  show antiferromagnetic transitions at 17 and 71 K, respectively.<sup>6</sup> In these compounds, the Ce and Pr ions are not in the trivalent state, but are rather tetravalent and the Ir ions are also tetravalent, which are quite different from the other  $Ba_2LnIrO_6$  and  $Ba_2LnMO_6$  ( $M = Nb, Ta, Ru$ ). Now, our attention has been focused on double perovskite oxides containing rhenium,  $Ba_2LnReO_6$ . In these compounds, the oxidation state of rhenium ions is expected to be in the pentavalent state. Their electronic configurations are  $[Xe]5d^2$  ( $[Xe]$ : xenon electronic

core), which is different from those for the above transition elements, *i.e.*, the  $Re^{5+}$  ion has two unpaired electrons. Therefore, the magnetic properties of  $Ba_2LnReO_6$  are expected to be quite different from those of other double perovskite oxides  $Ba_2LnMO_6$  ( $M = Nb, Ta, Ru, Ir$ ), because in general, the effect of  $M^{5+}$  ions on the magnetic properties of  $Ba_2LnMO_6$  is larger than that of  $Ln^{3+}$  ions. However, the magnetic properties of  $Ba_2LnReO_6$  have not been studied in detail.<sup>8</sup>

In this study, we have prepared  $Ba_2LnReO_6$  ( $Ln = Y, Nd, Sm-Lu$ ), and studied their crystal structures and magnetic properties through X-ray diffraction, magnetic susceptibility, and specific heat measurements.

## Experimental

### Sample preparation

As starting materials, powders of barium peroxide ( $BaO_2$ ), lanthanide sesquioxide ( $Ln_2O_3$ , except for  $Ln = Tb$ ), rhenium metal (Re), and rhenium dioxide ( $ReO_2$ ) were used. For the case of terbium,  $Tb_4O_7$  was used. Their purity is higher than 99.9%. In order to remove any moisture,  $Nd_2O_3$  was preheated in air at 1173 K. The stoichiometric mixtures were ground, pressed into pellets, and sealed in an evacuated silica tube. The pellets were annealed at 1073–1373 K for 6–24 h with several intervening regrinding and repelletizing steps.

A diamagnetic material  $Ba_2LuTaO_6$ , which is isomorphous with  $Ba_2LnReO_6$ , was also prepared. As will be described later, this compound is needed to estimate the lattice contribution of the specific heat to the total specific heat of  $Ba_2LnReO_6$ . Starting materials were  $BaCO_3$ ,  $Lu_2O_3$  and  $Ta_2O_5$ . These reagents were weighed in appropriate metal ratios and ground thoroughly in an agate mortar. The mixtures were pressed into pellets and were calcined at 1173 K. The calcined materials were reground and sintered in air at 1573 K for several days with intermediate regrinding and repelletizing.

### X-Ray diffraction

Powder X-ray diffraction measurements were carried out at room temperature in the range  $10 \leq 2\theta \leq 120$ , using a  $2\theta$  step size of  $0.02^\circ$  with  $CuK\alpha$  radiation on a multiflex diffractometer (Rigaku). Rietveld analyses were carried out with the program RIETAN 2000<sup>9</sup> using collected diffraction data.

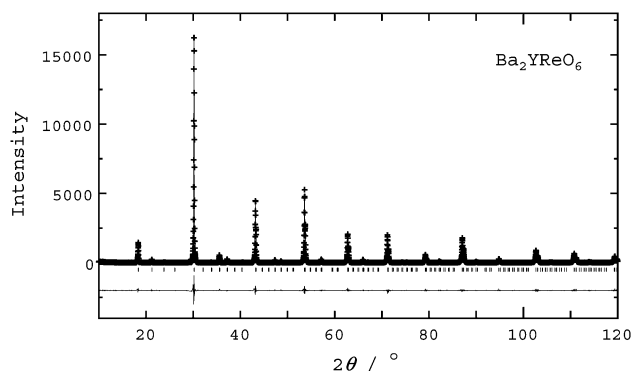


Fig. 1 Powder X-ray diffraction pattern of Ba<sub>2</sub>YReO<sub>6</sub>.

### Magnetic susceptibility

The temperature dependence of the magnetic susceptibilities was measured under both zero-field-cooled condition (ZFC) and field-cooled condition (FC) in the temperature range 2–300 K using a SQUID magnetometer (Quantum Design, MPMS-5S). The ZFC susceptibility measurements were performed under an applied magnetic field of 0.1 T, after the sample was cooled from 300 to 2K in a zero field. For the FC susceptibility measurements, the sample was cooled in the presence of a field of 0.1 T. The magnetization was measured at 5 K by changing the applied magnetic field between –5 and 5 T.

### Heat capacity

Heat capacity measurements were carried out using a relaxation technique supplied by commercial heat capacity measurement system (Quantum Design, PPMS) in the temperature range 2–300 K. The sample in the form of pellet was mounted on an alumina plate with Apiezon for better thermal contact.

## Results and discussion

### Crystal structures

The results of the powder X-ray diffraction measurements show that Ba<sub>2</sub>LnReO<sub>6</sub> (Ln = Y, Nd, Sm–Lu) compounds were formed as a single phase with a perovskite-type structure. For the case of Ln = La, Ce and Pr, a single perovskite phase was not formed, which is due to the large size of these lanthanides as the B-site ions. Fig. 1 shows the X-ray diffraction pattern of Ba<sub>2</sub>YReO<sub>6</sub>. Rietveld analysis was performed with the program RIETAN to obtain powder X-ray diffraction profiles. The structures were refined by applying the space group *P2<sub>1</sub>/n*. This space group allows two crystallographically distinct octahedral sites in the perovskite structure, thus permitting 1 : 1 positional ordering between the B site ions, Ln<sup>3+</sup> and Re<sup>5+</sup> ions. These ions are arranging alternately and they have a rock salt sublattice. Fig. 2 shows the crystal structure of Ba<sub>2</sub>LnReO<sub>6</sub>.

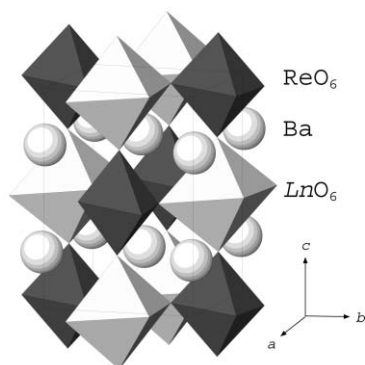


Fig. 2 Crystal structure of Ba<sub>2</sub>LnReO<sub>6</sub>.

The unit cell parameters and the reliability factors for Ba<sub>2</sub>LnReO<sub>6</sub> are listed in Table 1. The atomic positional parameters for Ba<sub>2</sub>YReO<sub>6</sub> after refinements are listed in Table 2.

Fig. 3 shows the variation of lattice parameters for the Ba<sub>2</sub>LnReO<sub>6</sub> with ionic radius of Ln<sup>3+</sup>.<sup>10</sup> As the ionic radius increases, the lattice parameters *a*, *b* and *c* increase. The variation is nearly linear, so it is thought that the oxidation state of the lanthanide is trivalent and that of rhenium is pentavalent for all Ba<sub>2</sub>LnReO<sub>6</sub> (Ln = Nd, Sm, Eu–Lu). Table 1 and Fig. 3 show that in the monoclinic region, the lattice parameter *β* increases and the differences among *a*, *b* and *c*/√2 spread with an increase of the Ln<sup>3+</sup> ionic radius. This result indicates that the crystal structures of Ba<sub>2</sub>LnReO<sub>6</sub> are more distorted from the cubic symmetry as the size of the Ln<sup>3+</sup> ion becomes larger.

Table 1 Unit cell parameters and *R* factors of Ba<sub>2</sub>LnReO<sub>6</sub> (Ln = Y, Nd, Sm–Lu)

Ln	<i>a</i> /Å	<i>b</i> /Å	<i>c</i> /Å	<i>β</i> /°	<i>R</i> <sub>wp</sub>	<i>R</i> <sub>1</sub>
Y	5.9205(7)	5.9202(7)	8.3750(2)	90.026(5)	14.89	3.34
Nd	6.0064(4)	6.0067(3)	8.5229(1)	90.045(2)	18.24	8.72
Sm	5.9847(7)	5.9868(7)	8.4685(5)	90.043(8)	17.87	6.18
Eu	5.9756(4)	5.9737(4)	8.4685(5)	90.00(2)	14.92	4.43
Gd	5.9602(3)	5.9638(4)	8.4329(3)	90.025(7)	15.87	4.53
Tb	5.944(1)	5.946(1)	8.4075(5)	90.02(1)	13.38	4.95
Dy	5.934(1)	5.933(1)	8.3910(2)	90.00(2)	15.37	3.00
Ho	5.921(1)	5.921(1)	8.3748(4)	90.00(2)	15.23	3.51
Er	5.9118(2)	5.9126(2)	8.3701(2)	90.00(4)	15.63	4.53
Tm	5.898(2)	5.898(2)	8.3417(2)	90.00(2)	11.89	4.44
Yb	5.890(6)	5.890(6)	8.300(1)	90.00(9)	13.91	2.57
Lu	5.880(1)	5.880(1)	8.3171(4)	90.01(5)	14.62	3.11

<sup>a</sup>*R*<sub>wp</sub> = [∑<sub>k</sub> w<sub>k</sub> |I<sub>k</sub>(obs) – I<sub>k</sub>(calc)|<sup>2</sup> / ∑<sub>k</sub> w<sub>k</sub> I<sub>k</sub>(obs)]<sup>1/2</sup>, *R*<sub>1</sub> = ∑<sub>k</sub> |I<sub>k</sub>(obs) – I<sub>k</sub>(calc)| / ∑<sub>k</sub> I<sub>k</sub>(obs).

Table 2 Structural parameters for Ba<sub>2</sub>YReO<sub>6</sub>

Atom	Site	<i>x</i>	<i>y</i>	<i>z</i>	<i>B</i> /Å <sup>2</sup>
Ba <sub>2</sub> YReO <sub>6</sub> space group: <i>P2<sub>1</sub>/n</i>					
Ba	4e	0.003(4)	0.002(1)	0.243(1)	0.51(6)
La	2d	1/2	0	0	0.1(2)
Re	2c	1/2	0	1/2	0.1(1)
O(1)	4e	0.24(3)	0.26(3)	0.00(4)	0.8(3)
O(2)	4e	0.21(3)	–0.29(3)	0.00(2)	0.8(3)
O(3)	4e	0.01(4)	0.51(1)	0.241(5)	0.8(3)

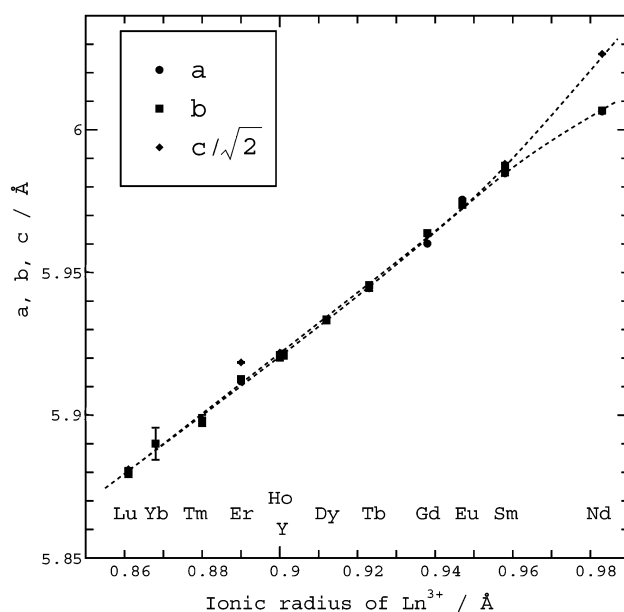
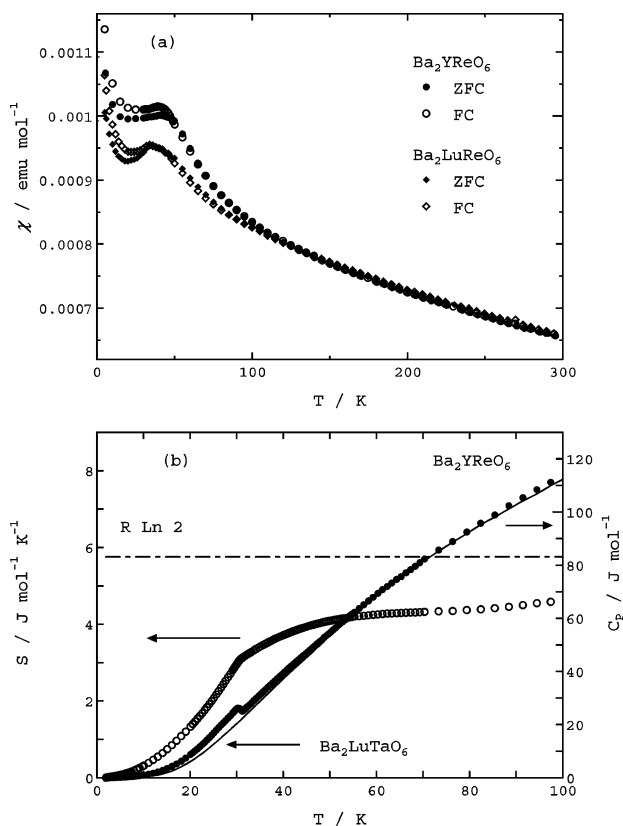


Fig. 3 Variation of lattice parameters for Ba<sub>2</sub>LnReO<sub>6</sub> (Ln = Y, Nd, Sm–Lu) with Ln<sup>3+</sup> radius.

## Magnetic properties

The molar magnetic susceptibilities of  $\text{Ba}_2\text{LnReO}_6$  ( $\text{Ln} = \text{Y}$ , lanthanides) are plotted as a function of temperature in Fig. 4–7(a) and Fig. 8 and 9. A magnetic anomaly is found for  $\text{Ln} = \text{Y}$ , Nd, Sm, Tb and Lu at 31, 6, 103, 2.5 and 33 K, respectively. They seem to be antiferromagnetic. In  $\text{Ba}_2\text{YReO}_6$ , the discrepancy in the observed transition temperatures between magnetic susceptibility and specific heat measurements is found (see Fig. 4), and the reason for this is not clear at present. In this study we adopt 31 K as the transition temperature, because a clear  $\lambda$ -type specific heat anomaly has been observed at 31 K. The Curie–Weiss law is valid for the magnetic susceptibilities of  $\text{Ba}_2\text{LnReO}_6$  except for those of  $\text{Ba}_2\text{SmReO}_6$  and  $\text{Ba}_2\text{EuReO}_6$  in higher temperature ranges ( $T > 150$  K). The effective magnetic moments ( $\mu_{\text{eff}}$ ) and Weiss constants ( $\theta$ ) of these compounds are listed in Table 3. The effective magnetic moments of  $\text{Ba}_2\text{YReO}_6$  and  $\text{Ba}_2\text{LuReO}_6$ , in which only the  $\text{Re}^{5+}$  ion is magnetic, are 2.32 and 2.30  $\mu_{\text{B}}$ , respectively. The calculated magnetic moment for a spin-only value ( $\text{Re}^{5+} : [\text{Xe}]5d^2$ ) is 2.83  $\mu_{\text{B}}$ . We consider that due to the effect of the crystal field, the orbital angular momentum has also contributed to the magnetic properties of these compounds, so the effective magnetic moments are smaller than the spin-only value. For other compounds, not only the  $\text{Re}^{5+}$  ion but also the  $\text{Ln}^{3+}$  ion is magnetic. When we assume that the magnetic moment of the  $\text{Re}^{5+}$  ion is 2.30  $\mu_{\text{B}}$  (which is close to those of  $\text{Ba}_2\text{LuReO}_6$  and  $\text{Ba}_2\text{YReO}_6$ ), the effective magnetic moments of  $\text{Ba}_2\text{LnReO}_6$  ( $\mu_{\text{calc}}$ ) are calculated from the equation  $\mu_{\text{calc}}^2 = \mu_{\text{eff}}(\text{Ln}^{3+})^2 + \mu_{\text{eff}}(\text{Re}^{5+})^2$ . They are also listed in Table 3 and agree with the moments experimentally obtained for  $\text{Ba}_2\text{LnReO}_6$  ( $\mu_{\text{exp}}$ ). The negative Weiss constants ( $\theta$ )



**Fig. 4** (a) Temperature dependence of the ZFC (filled symbols) and FC (open symbols) molar magnetic susceptibilities for  $\text{Ba}_2\text{YReO}_6$  (●, ○) and  $\text{Ba}_2\text{LuReO}_6$  (◆, ◇). (b) Temperature dependence of specific heat (filled circle) and magnetic entropy (open circle) for  $\text{Ba}_2\text{YReO}_6$ . The solid line shows temperature dependence of specific heat for  $\text{Ba}_2\text{LuTaO}_6$ .

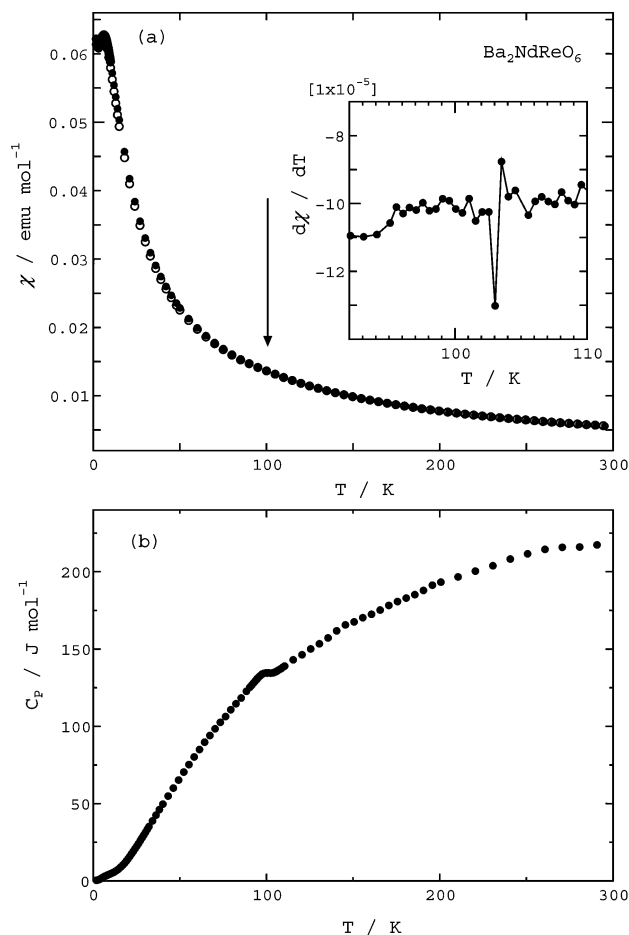


**Fig. 5** (a) Temperature dependence of the ZFC (filled circle) and FC (open circle) molar magnetic susceptibilities for  $\text{Ba}_2\text{NdReO}_6$ . The arrow shows the magnetic anomaly temperature. The inset displays the temperature derivative of molar magnetic susceptibilities. (b) Temperature dependence of specific heat (filled circle) for  $\text{Ba}_2\text{NdReO}_6$ .

indicate that the predominant magnetic interactions in these compounds are antiferromagnetic.

The divergence between the FC and ZFC susceptibilities has been observed for  $\text{Ba}_2\text{LnReO}_6$  ( $\text{Ln} = \text{Y}$ , Sm, Lu) (see Fig. 4 and 6). Fig. 10 shows the variation of magnetization as a function of magnetic field for  $\text{Ba}_2\text{LuReO}_6$  at 5 K. Small magnetic hysteresis has been found. These results indicate that the above  $\text{Ba}_2\text{LnReO}_6$  compounds are not ideal antiferromagnets. We consider that this is due to the results of a low crystal symmetry of these compounds (*i.e.*, monoclinic symmetry). That is, the Dzyaloshinsky–Moriya (D–M) interaction can exist between the magnetically ordered elements, which results in the existence of a weak ferromagnetic component in their susceptibilities. The  $\text{Ba}_2\text{EuReO}_6$  and  $\text{Ba}_2\text{SmReO}_6$  shows that the temperature dependence of magnetic susceptibility does not obey the Curie–Weiss law. The ground state  $^7F_0$  of  $\text{Eu}^{3+}$  is nonmagnetic, and the excited states  $^7F_J$  ( $J = 1, 2, \dots, 6$ ) are close enough to give energy differences comparable to  $k_{\text{B}}T$  at room temperature. The excitation to the upper states affects sufficiently the magnetic susceptibility at room temperature. Thus, the molar magnetic susceptibility for  $\text{Eu}^{3+}$  can be expressed by the following equation<sup>11</sup>:

$$\chi_{\text{M}}(\text{Eu}^{3+}) = \frac{N_{\text{A}}\mu_{\text{B}}^2/3k_{\text{B}}}{\gamma T} \times \frac{24 + (13.5\gamma - 1.5)e^{-\gamma} + (67.5\gamma - 2.5)e^{-3\gamma} + (189\gamma - 3.5)e^{-6\gamma}}{1 + 3e^{-\gamma} + 5e^{-3\gamma} + 7e^{-6\gamma}} \quad (1)$$

where the parameter  $\gamma = \lambda/k_{\text{B}}T$  is the ratio of the multiplet

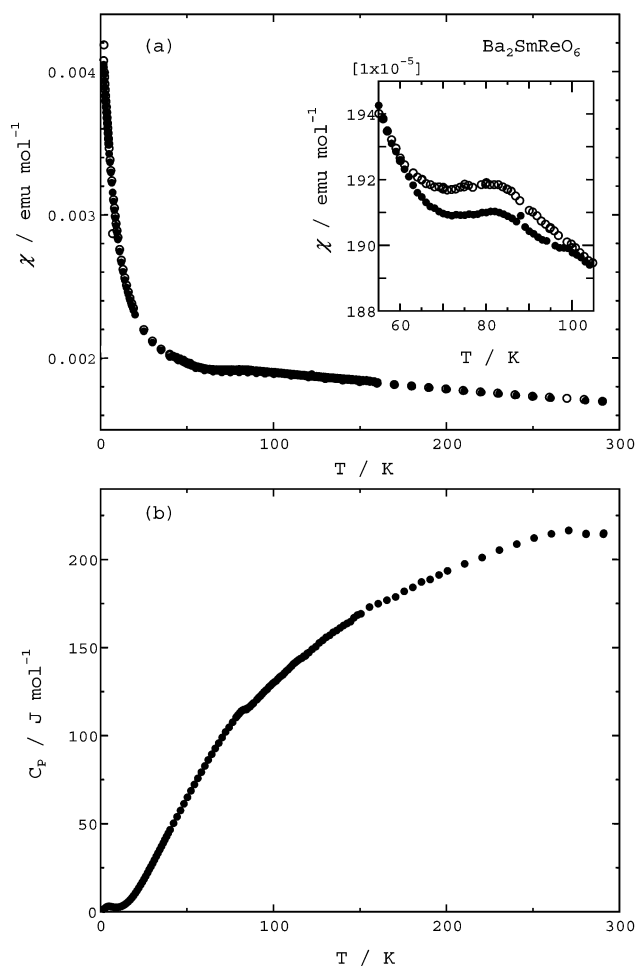


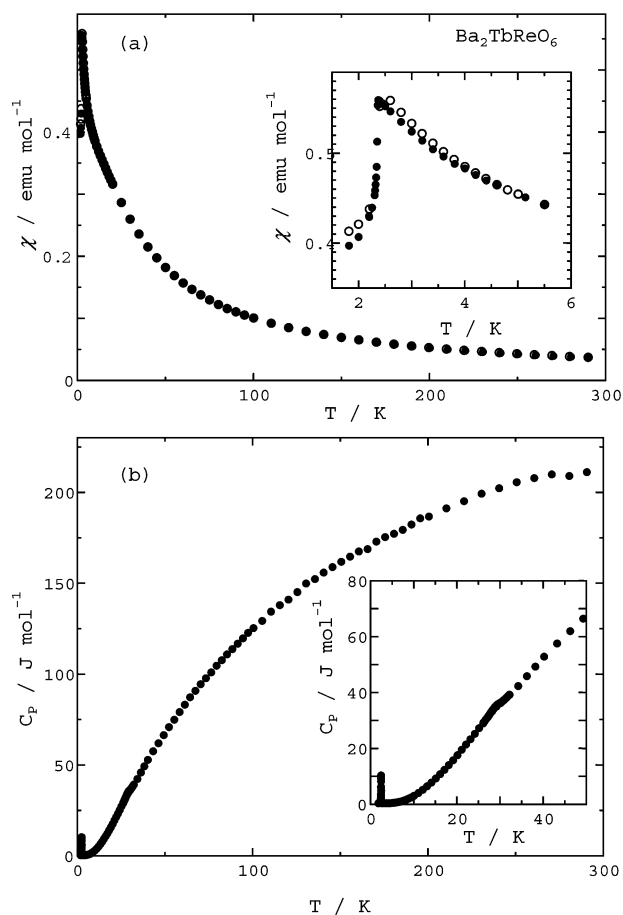
**Fig. 6** (a) Temperature dependence of the ZFC (filled circle) and FC (open circle) molar magnetic susceptibilities for  $\text{Ba}_2\text{SmReO}_6$ . The inset shows the detailed susceptibilities in the temperature range of 55–105 K. (b) Temperature dependence of specific heat (filled circle) for  $\text{Ba}_2\text{SmReO}_6$ .

width (the spin-orbit coupling constant,  $\lambda$ ) and the thermal energy ( $k_B T$ ), and  $\gamma$  is 1/21 for the  $\text{Eu}^{3+}$  ion. We consider that in the paramagnetic region, the magnetic behavior of the  $\text{Eu}^{3+}$  ion and  $\text{Re}^{5+}$  ion are independent of each other and that the susceptibility of  $\text{Ba}_2\text{EuReO}_6$  will be given by the sum of the susceptibilities of each paramagnetic ion. If we assume that the susceptibility of  $\text{Re}^{5+}$  follows the Curie–Weiss law, the total magnetic susceptibility of  $\text{Ba}_2\text{EuReO}_6$  will be given by

$$\chi_M = \chi_M(\text{Eu}^{3+}) + \frac{C}{T - \theta} + \chi_{\text{TIP}} \quad (2)$$

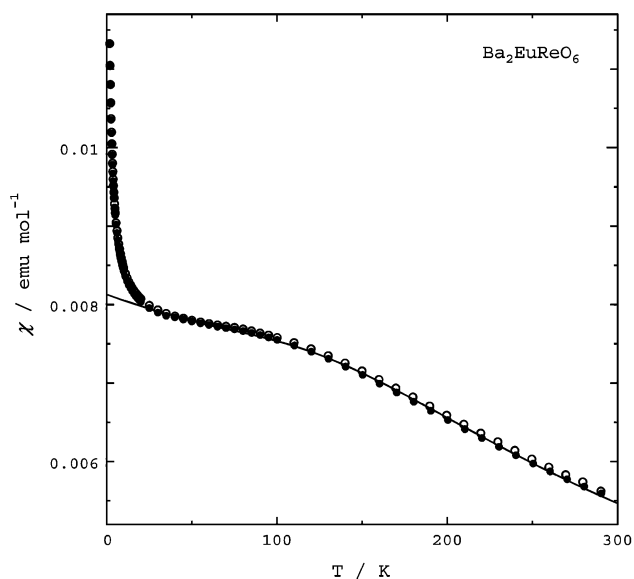
where  $C$  is the Curie constant for  $\text{Re}^{5+}$  and  $\chi_{\text{TIP}}$  is the temperature-independent susceptibility of  $\text{Ba}_2\text{EuReO}_6$ . In order to explain the behavior of magnetic susceptibility and to estimate the effective magnetic moment and Weiss constant of  $\text{Re}^{5+}$ , we attempted to fit this equation to experimental susceptibilities. To prevent the parameters from converging to meaningless values, we fixed the Curie constant values to 0.66, which is close to the values for  $\text{Ba}_2\text{YReO}_6$  and  $\text{Ba}_2\text{LuReO}_6$ . By fitting, we have obtained  $\lambda = 349 \text{ cm}^{-1}$  and  $\theta = -289.5 \text{ K}$ . This  $\lambda$  value is close to the values reported in other ordered perovskites, for example,  $339 \text{ cm}^{-1}$  ( $\text{Ba}_2\text{EuNbO}_6$ )<sup>1</sup>,  $364 \text{ cm}^{-1}$  ( $\text{Ba}_2\text{EuIrO}_6$ )<sup>6</sup> and  $332 \text{ cm}^{-1}$  ( $\text{Ba}_2\text{EuTaO}_6$ ).<sup>2</sup> We attempted the same fitting for the susceptibilities of  $\text{Ba}_2\text{SmReO}_6$ , but the calculation did not converge. This is because of magnetic anomaly found at a relatively high temperature.

Fig. 4–7(b) show the variation of the heat capacity for  $\text{Ba}_2\text{LnReO}_6$  as a function of temperature. The data for  $\text{Ba}_2\text{LnReO}_6$  ( $\text{Ln} = \text{Y}, \text{Nd}, \text{Sm}, \text{Gd}, \text{Dy}, \text{Ho}$  and  $\text{Lu}$ ) show a



**Fig. 7** (a) Temperature dependence of the ZFC (filled circle) and FC (open circle) molar magnetic susceptibilities for  $\text{Ba}_2\text{TbReO}_6$ . The inset shows the detailed susceptibilities in the temperature range 1.8–5.5 K. (b) Temperature dependence of specific heat (solid circle) for  $\text{Ba}_2\text{TbReO}_6$ . The inset shows the detailed specific heat in the temperature range of 1.8–50 K.

heat capacity anomaly at low temperatures, and  $\text{Ba}_2\text{TbReO}_6$  shows two heat capacity anomalies. The anomaly temperatures are consistent with the magnetic transition temperatures in magnetic susceptibility curves and they are listed in Table 3. No specific heat capacity anomaly has been observed down to 2.0 K



**Fig. 8** Temperature dependence of the magnetic susceptibility of  $\text{Ba}_2\text{EuReO}_6$ . A solid line is calculated with eqn. (2).

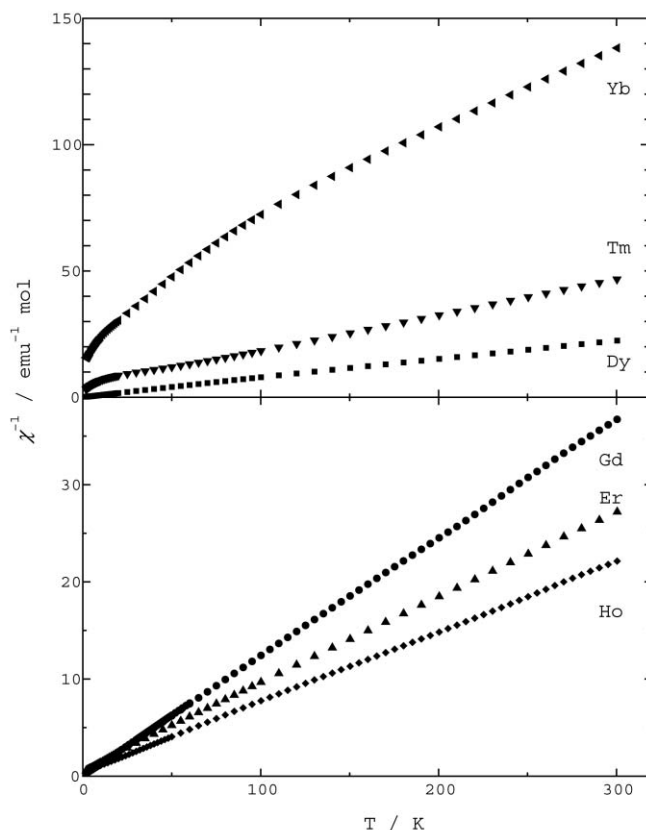


Fig. 9 Temperature dependence of the inverse magnetic susceptibilities of  $\text{Ba}_2\text{LnReO}_6$  ( $\text{Ln} = \text{Gd}, \text{Dy}, \text{Ho}, \text{Er}, \text{Tm}$  and  $\text{Yb}$ ).

for  $\text{Ba}_2\text{LnReO}_6$  with  $\text{Ln} = \text{Eu}, \text{Er}, \text{Tm}$  and  $\text{Yb}$ , which is consistent with the results of the magnetic susceptibility measurements. In Fig. 4(b), the results of the specific heat measurements for  $\text{Ba}_2\text{LuTaO}_6$ , which has no paramagnetic ion, are also shown by the solid line. If we assume that the electronic and lattice contributions to the specific heat are equal between  $\text{Ba}_2\text{LnReO}_6$  and  $\text{Ba}_2\text{LuTaO}_6$ , the magnetic specific heat for  $\text{Ba}_2\text{LnReO}_6$  is obtained by subtracting the specific heat of  $\text{Ba}_2\text{LuTaO}_6$  from that of  $\text{Ba}_2\text{LnReO}_6$ . From the temperature dependence of the magnetic specific heat, the magnetic entropy change of  $\text{Ba}_2\text{YReO}_6$  is calculated as shown in Fig. 4(b). The magnetic entropy changes of  $\text{Ba}_2\text{YReO}_6$  and  $\text{Ba}_2\text{LuReO}_6$  at 100 K are 4.6 and 4.7  $\text{J}(\text{mol K})^{-1}$ , respectively. It is expected that the magnetic entropy change of  $\text{Re}^{5+}$  is  $R\ln(2S+1) = 9.13 \text{ J}(\text{mol K})^{-1}$ , where  $R$  and  $S$  are the molar gas constant and the spin quantum number, respectively. It is thought that due to the effect of the crystal field, the magnetic entropy decreases. In an octahedral crystal field environment, the ground state of the  $\text{Re}^{5+}$  ion ( $5d^2$ , the state  ${}^3\text{F}_2$ ) degenerate to five-fold ( $\Gamma_3 + \Gamma_5$ ).

**Table 3** Experimental effective magnetic moments ( $\mu_{\text{exp}}$ ), calculated magnetic moments ( $\mu_{\text{calc}}^2 = \mu_{\text{eff}}(\text{Ln}^{3+})^2 + \mu_{\text{eff}}(\text{Re}^{5+})^2$ ), Weiss constants ( $\theta$ ) and magnetic transition temperatures ( $T_N$ ) for  $\text{Ba}_2\text{LnReO}_6$  ( $\text{Ln} = \text{Y}, \text{Nd}, \text{Sm-Lu}$ )

$\text{Ln}$	$\mu_{\text{exp}}/\mu_B$	$\mu_{\text{calc}}/\mu_B$	$\theta$	$T_N$
Y	2.32	—	-726	31
Nd	3.86	4.29	-35.2	100
Sm	—	2.45	—	82
Eu	—	2.30	—	—
Gd	8.10	8.27	-1.9	65
Tb	9.48	9.99	-14.1	2.4, 29
Dy	10.51	10.88	-10.0	70
Ho	10.52	10.83	-7.4	27
Er	9.56	9.86	-10.9	—
Tm	7.49	7.89	-26.9	—
Yb	5.04	5.09	-138	—
Lu	2.30	—	-703	33

In the case of lower symmetry, the degeneracy is lifted and the ground state becomes doublet ( $\Gamma_3$ ). Thus the magnetic entropy change is  $R\ln 2 = 5.76 \text{ J}(\text{mol K})^{-1}$ . Although this assumption is correct, the magnetic entropy change is still lower. It might be ascribed to the beginning of magnetic transition at higher temperature.

For  $\text{Ln} = \text{Sm}$  and  $\text{Nd}$ , heat capacity anomalies, corresponding to magnetic anomalies found in the magnetic susceptibility curve, were also observed. It is suggested that the anomalies are based on the magnetic transition of  $\text{Re}^{5+}$ .

For  $\text{Ln} = \text{Gd}, \text{Tb}, \text{Dy}$  and  $\text{Ho}$ , heat capacity anomalies are also observed at 65, 29, 70 and 27 K, respectively, as is the case with  $\text{Ba}_2\text{SmReO}_6$  and  $\text{Ba}_2\text{NdReO}_6$ . However, no magnetic

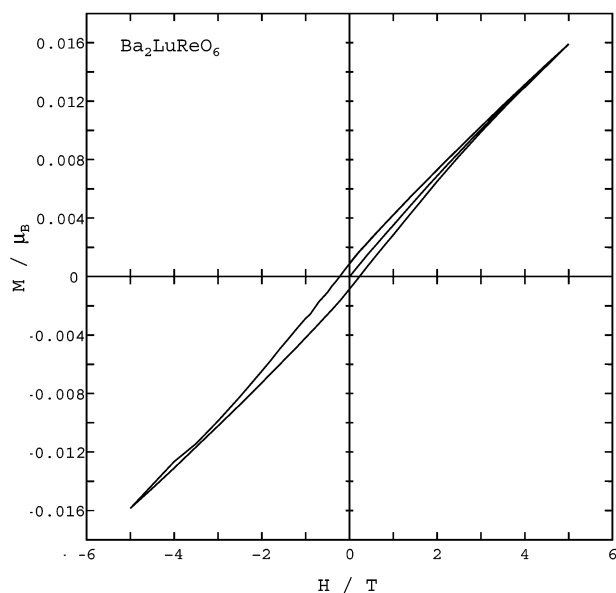


Fig. 10 Field-dependence of the magnetization for  $\text{Ba}_2\text{LuReO}_6$  at 5 K.

anomaly is observed in the magnetic susceptibility curve since the contribution of the magnetic moment of the  $\text{Re}^{5+}$  ion to the behavior of  $\text{Ba}_2\text{LnReO}_6$  ( $\text{Ln} = \text{Gd}, \text{Tb}, \text{Dy}$  and  $\text{Ho}$ ) is smaller compared with that of the  $\text{Ln}^{3+}$  ion. The heat capacity anomalies might be based on magnetic transition of  $\text{Re}^{5+}$ .

$\text{Ba}_2\text{TbReO}_6$  shows a heat capacity anomaly also at 2.5 K, corresponding to the magnetic anomaly found in the magnetic susceptibility curve. It is thought that this anomaly is based on the magnetic transition of  $\text{Tb}^{3+}$ .

In conclusion, we have found that  $\text{Ba}_2\text{ReLnO}_6$  ( $\text{Ln} = \text{Y}, \text{Nd}, \text{Sm}, \text{Gd}, \text{Tb}, \text{Dy}, \text{Ho}, \text{Lu}$ ) show magnetic transitions at low temperatures which vary with the  $\text{Ln}^{3+}$  ion. They might be the antiferromagnetic transition of the  $\text{Re}^{5+}$  ion.  $\text{Ba}_2\text{TbReO}_6$  shows the magnetic transition due to the antiferromagnetic transition of the  $\text{Tb}^{3+}$  ion. On the other hand,  $\text{Ba}_2\text{LnReO}_6$  ( $\text{Ln} = \text{Eu}, \text{Er}, \text{Tm}$  and  $\text{Yb}$ ) are paramagnetic down to 1.8 K.

It should be noticed that the magnetic transition temperatures for the compounds with  $\text{Ln} = \text{Nd}, \text{Sm}, \text{Gd}, \text{Dy}$  are much higher than those for the compounds with  $\text{Ln} = \text{Y}, \text{Lu}$ , although these magnetic transitions could be due to antiferromagnetic interactions between the same  $\text{Re}^{5+}$  ions. To fully understand the nature of the transition, it is necessary to

perform single crystal growth and microscopic measurements such as neutron diffraction and NMR.

## References

- 1 K. Henmi, Y. Hinatsu and N. Masaki, *J. Solid State Chem.*, 1999, **148**, 353.
- 2 Y. Doi and Y. Hinatsu, *J. Phys.: Condens. Matter*, 2001, **13**, 4191.
- 3 N. Taira and Y. Hinatsu, *J. Solid State Chem.*, 2000, **150**, 31.
- 4 Y. Izumiyama, Y. Doi, M. Wakeshima, Y. Hinatsu, Y. Shimojo and Y. Morii, *J. Phys.: Condens. Matter*, 2001, **13**, 1303.
- 5 Y. Izumiyama, Y. Doi, M. Wakeshima, Y. Hinatsu, K. Oikawa, Y. Shimojo and Y. Morii, *J. Mater. Chem.*, 2000, **10**, 2364.
- 6 M. Wakeshima, D. Harada and Y. Hinatsu, *J. Mater. Chem.*, 2000, **10**, 419.
- 7 M. Wakeshima, D. Harada, Y. Hinatsu and N. Masaki, *J. Solid State Chem.*, 1999, **147**, 618.
- 8 B. Gilbert and M. Capestan, *Bull. Soc. Chim. Fr.*, 1969, **6**, 1872.
- 9 F. Izumi, *The Rietveld Method*, ed. R. A. Young, Oxford University Press, Oxford, 1993, ch. 13.
- 10 R. D. Shannon, *Acta Crystallogr., Sect. A*, 1976, **32**, 751.
- 11 J. H. Van Vleck, *The Theory of Electric and Magnetic Susceptibilities*, Clarendon, Oxford, 1932.